

Search for the Decays $B_s^0, B_d^0 \rightarrow e^\pm \mu^\mp$ and Pati-Salam Leptoquarks

- F. Abe,¹⁷ H. Akimoto,³⁹ A. Akopian,³¹ M. G. Albrow,⁷ A. Amadon,⁵ S. R. Amendolia,²⁷ D. Amidei,²⁰ J. Antos,³³
 S. Aota,³⁷ G. Apollinari,³¹ T. Arisawa,³⁹ T. Asakawa,³⁷ W. Ashmanskas,¹⁸ M. Atac,⁷ P. Azzi-Bacchetta,²⁵
 N. Bacchetta,²⁵ S. Bagdasarov,³¹ M. W. Bailey,²² P. de Barbaro,³⁰ A. Barbaro-Galtieri,¹⁸ V. E. Barnes,²⁹
 B. A. Barnett,¹⁵ M. Barone,⁹ G. Bauer,¹⁹ T. Baumann,¹¹ F. Bedeschi,²⁷ S. Behrends,³ S. Belforte,²⁷ G. Bellettini,²⁷
 J. Bellinger,⁴⁰ D. Benjamin,³⁵ J. Bensinger,³ A. Beretvas,⁷ J. P. Berge,⁷ J. Berryhill,⁵ S. Bertolucci,⁹ S. Bettelli,²⁷
 B. Bevensee,²⁶ A. Bhatti,³¹ K. Biery,⁷ C. Bigongiari,²⁷ M. Binkley,⁷ D. Bisello,²⁵ R. E. Blair,¹ C. Blocker,³
 K. Bloom,²⁰ S. Blusk,³⁰ A. Bodek,³⁰ W. Bokhari,²⁶ G. Bolla,²⁹ Y. Bonushkin,⁴ D. Bortoletto,²⁹ J. Boudreau,²⁸
 L. Breccia,² C. Bromberg,²¹ N. Bruner,²² R. Brunetti,² E. Buckley-Geer,⁷ H. S. Budd,³⁰ K. Burkett,¹¹ G. Busetto,²⁵
 A. Byon-Wagner,⁷ K. L. Byrum,¹ M. Campbell,²⁰ A. Caner,²⁷ W. Carithers,¹⁸ D. Carlsmith,⁴⁰ J. Cassada,³⁰
 A. Castro,²⁵ D. Cauz,³⁶ A. Cerri,²⁷ P. S. Chang,³³ P. T. Chang,³³ H. Y. Chao,³³ J. Chapman,²⁰ M.-T. Cheng,³³
 M. Chertok,³⁴ G. Chiarelli,²⁷ C. N. Chiou,³³ F. Chlebana,⁷ L. Christofek,¹³ R. Cropp,¹⁴ M. L. Chu,³³ S. Cihangir,⁷
 A. G. Clark,¹⁰ M. Cobal,²⁷ E. Cocca,²⁷ M. Contreras,⁵ J. Conway,³² J. Cooper,⁷ M. Cordelli,⁹ D. Costanzo,²⁷
 C. Couyoumtzelis,¹⁰ D. Cronin-Hennessy,⁶ R. Culbertson,⁵ D. Dagenhart,³⁸ T. Daniels,¹⁹ F. DeJongh,⁷
 S. Dell'Agnello,⁹ M. Dell'Orso,²⁷ R. Demina,⁷ L. Demortier,³¹ M. Deninno,² P. F. Derwent,⁷ T. Devlin,³²
 J. R. Dittmann,⁶ S. Donati,²⁷ J. Done,³⁴ T. Dorigo,²⁵ N. Eddy,¹³ K. Einsweiler,¹⁸ J. E. Elias,⁷ R. Ely,¹⁸ E. Engels, Jr.,²⁸
 W. Erdmann,⁷ D. Errede,¹³ S. Errede,¹³ Q. Fan,³⁰ R. G. Feild,⁴¹ Z. Feng,¹⁵ C. Ferretti,²⁷ I. Fiori,² B. Flaughier,⁷
 G. W. Foster,⁷ M. Franklin,¹¹ J. Freeman,⁷ J. Friedman,¹⁹ H. Frisch,⁵ Y. Fukui,¹⁷ S. Gadomski,¹⁴ S. Galeotti,²⁷
 M. Gallinaro,²⁶ O. Ganel,³⁵ M. Garcia-Sciveres,¹⁸ A. F. Garfinkel,²⁹ C. Gay,⁴¹ S. Geer,⁷ D. W. Gerdes,¹⁵ P. Giannetti,²⁷
 N. Giokaris,³¹ P. Giromini,⁹ G. Giusti,²⁷ M. Gold,²² A. Gordon,¹¹ A. T. Goshaw,⁶ Y. Gotra,²⁸ K. Goulianios,³¹
 H. Grassmann,³⁶ L. Groer,³² C. Gross-Pilcher,⁵ G. Guillian,²⁰ J. Guimaraes da Costa,¹⁵ R. S. Guo,³³ C. Haber,¹⁸
 E. Hafen,¹⁹ S. R. Hahn,⁷ R. Hamilton,¹¹ T. Handa,¹² R. Handler,⁴⁰ F. Happacher,⁹ W. Hao,³⁵ K. Hara,³⁷
 A. D. Hardman,²⁹ R. M. Harris,⁷ F. Hartmann,¹⁶ J. Hauser,⁴ E. Hayashi,³⁷ J. Heinrich,²⁶ A. Heiss,¹⁶ B. Hinrichsen,¹⁴
 K. D. Hoffman,²⁹ M. Hohlmann,⁵ C. Holck,²⁶ R. Hollebeek,²⁶ L. Holloway,¹³ Z. Huang,²⁰ B. T. Huffman,²⁸
 R. Hughes,²³ J. Huston,²¹ J. Huth,¹¹ H. Ikeda,³⁷ M. Incagli,²⁷ J. Incandela,⁷ G. Introzzi,²⁷ J. Iwai,³⁹ Y. Iwata,¹²
 E. James,²⁰ H. Jensen,⁷ U. Joshi,⁷ E. Kajfasz,²⁵ H. Kambara,¹⁰ T. Kaneko,³⁴ T. Kaneko,³⁷ K. Karr,³⁸ H. Kasha,⁴¹
 Y. Kato,²⁴ T. A. Keaffaber,²⁹ K. Kelley,¹⁹ R. D. Kennedy,⁷ R. Kephart,⁷ D. Kestenbaum,¹¹ D. Khazins,⁶ T. Kikuchi,³⁷
 B. J. Kim,²⁷ H. S. Kim,¹⁴ S. H. Kim,³⁷ Y. K. Kim,¹⁸ L. Kirsch,³ S. Klimenko,⁸ D. Knoblauch,¹⁶ P. Koehn,²³
 A. Köngeter,¹⁶ K. Kondo,³⁷ J. Konigsberg,⁸ K. Kordas,¹⁴ A. Korytov,⁸ E. Kovacs,¹ W. Kowald,⁶ J. Kroll,²⁶
 M. Kruse,³⁰ S. E. Kuhlmann,¹ E. Kuns,³² K. Kurino,¹² T. Kuwabara,³⁷ A. T. Laasanen,²⁹ S. Lami,²⁷ S. Lammel,⁷
 J. I. Lamoureux,³ M. Lancaster,¹⁸ M. Lanzoni,²⁷ G. Latino,²⁷ T. LeCompte,¹ S. Leone,²⁷ J. D. Lewis,⁷ M. Lindgren,⁴
 T. M. Liss,¹³ J. B. Liu,³⁰ Y. C. Liu,³³ N. Lockyer,²⁶ O. Long,²⁶ C. Loomis,³² M. Loretta,²⁵ D. Lucchesi,²⁷ P. Lukens,⁷
 S. Lusin,⁴⁰ J. Lys,¹⁸ K. Maeshima,⁷ P. Maksimovic,¹¹ M. Mangano,²⁷ M. Mariotti,²⁵ J. P. Marriner,⁷ G. Martignon,²⁵
 A. Martin,⁴¹ J. A. J. Matthews,²² P. Mazzanti,² K. McFarland,³⁰ P. McIntyre,³⁴ P. Melese,³¹ M. Menguzzato,²⁵
 A. Menzione,²⁷ E. Meschi,²⁷ S. Metzler,²⁶ C. Miao,²⁰ T. Miao,⁷ G. Michail,¹¹ R. Miller,²¹ H. Minato,³⁷ S. Miscetti,⁹
 M. Mishina,¹⁷ S. Miyashita,³⁷ N. Moggi,²⁷ E. Moore,²² Y. Morita,¹⁷ A. Mukherjee,⁷ T. Muller,¹⁶ P. Murat,²⁷
 S. Murgia,²¹ M. Musy,³⁶ H. Nakada,³⁷ T. Nakaya,⁵ I. Nakano,¹² C. Nelson,⁷ D. Neuberger,¹⁶ C. Newman-Holmes,⁷
 C.-Y. P. Ngan,¹⁹ L. Nodulman,¹ A. Nomerotski,⁸ S. H. Oh,⁶ T. Ohmoto,¹² T. Ohsugi,¹² R. Oishi,³⁷ M. Okabe,³⁷
 T. Okusawa,²⁴ J. Olsen,⁴⁰ C. Pagliarone,²⁷ R. Paoletti,²⁷ V. Papadimitriou,³⁵ S. P. Pappas,⁴¹ N. Parashar,²⁷ A. Parri,⁹
 J. Patrick,⁷ G. Pauletta,³⁶ M. Paulini,¹⁸ A. Perazzo,²⁷ L. Pescara,²⁵ M. D. Peters,¹⁸ T. J. Phillips,⁶ G. Piacentino,²⁷
 M. Pillai,³⁰ K. T. Pitts,⁷ R. Plunkett,⁷ A. Pompos,²⁹ L. Pondrom,⁴⁰ J. Proudfoot,¹ F. Ptohos,¹¹ G. Punzi,²⁷ K. Ragan,¹⁴
 D. Reher,¹⁸ M. Reischl,¹⁶ A. Ribon,²⁵ F. Rimondi,² L. Ristori,²⁷ W. J. Robertson,⁶ A. Robinson,¹⁴ T. Rodrigo,²⁷
 S. Rolli,³⁸ L. Rosenson,¹⁹ R. Roser,¹³ T. Saab,¹⁴ W. K. Sakamoto,³⁰ D. Saltzberg,⁴ A. Sansoni,⁹ L. Santi,³⁶ H. Sato,³⁷
 P. Schlabach,⁷ E. E. Schmidt,⁷ M. P. Schmidt,⁴¹ A. Scott,⁴ A. Scribano,²⁷ S. Segler,⁷ S. Seidel,²² Y. Seiya,³⁷
 F. Semeria,² T. Shah,¹⁹ M. D. Shapiro,¹⁸ N. M. Shaw,²⁹ P. F. Shepard,²⁸ T. Shibayama,³⁷ M. Shimojima,³⁷ M. Shochet,⁵
 J. Siegrist,¹⁸ A. Sill,³⁵ P. Sinervo,¹⁴ P. Singh,¹³ K. Sliwa,³⁸ C. Smith,¹⁵ F. D. Snider,¹⁵ J. Spalding,⁷ T. Speer,¹⁰
 P. Sphicas,¹⁹ F. Spinella,²⁷ M. Spiropulu,¹¹ L. Spiegel,⁷ L. Stanco,²⁵ J. Steele,⁴⁰ A. Stefanini,²⁷ R. Ströhmer,^{7,*}
 J. Strologas,¹³ F. Strumia,¹⁰ D. Stuart,⁷ K. Sumorok,¹⁹ J. Suzuki,³⁷ T. Suzuki,³⁷ T. Takahashi,²⁴ T. Takano,²⁴
 R. Takashima,¹² K. Takikawa,³⁷ M. Tanaka,³⁷ B. Tannenbaum,⁴ F. Tartarelli,²⁷ W. Taylor,¹⁴ M. Tecchio,²⁰
 P. K. Teng,³³ Y. Teramoto,²⁴ K. Terashi,³⁷ S. Tether,¹⁹ D. Theriot,⁷ T. L. Thomas,²² R. Thurman-Keup,¹ M. Timko,³⁸

P. Tipton,³⁰ A. Titov,³¹ S. Tkaczyk,⁷ D. Toback,⁵ K. Tollefson,³⁰ A. Tollestrup,⁷ H. Toyoda,²⁴ W. Trischuk,¹⁴ J. F. de Troconiz,¹¹ S. Truitt,²⁰ J. Tseng,¹⁹ N. Turini,²⁷ T. Uchida,³⁷ F. Ukegawa,²⁶ J. Valls,³² S. C. van den Brink,²⁸ S. Vejcik III,²⁰ G. Velev,²⁷ R. Vidal,⁷ R. Vilar,^{7,*} D. Vucinic,¹⁹ R. G. Wagner,¹ R. L. Wagner,⁷ J. Wahl,⁵ N. B. Wallace,²⁷ A. M. Walsh,³² C. Wang,⁶ C. H. Wang,³³ M. J. Wang,³³ A. Warburton,¹⁴ T. Watanabe,³⁷ T. Watts,³² R. Webb,³⁴ C. Wei,⁶ H. Wenzel,¹⁶ W. C. Wester III,⁷ A. B. Wicklund,¹ E. Wicklund,⁷ R. Wilkinson,²⁶ H. H. Williams,²⁶ P. Wilson,⁷ B. L. Winer,²³ D. Winn,²⁰ D. Wolinski,²⁰ J. Wolinski,²¹ S. Worm,²² X. Wu,¹⁰ J. Wyss,²⁷ A. Yagil,⁷ W. Yao,¹⁸ K. Yasuoka,³⁷ G. P. Yeh,⁷ P. Yeh,³³ J. Yoh,⁷ C. Yosef,²¹ T. Yoshida,²⁴ I. Yu,⁷ A. Zanetti,³⁶ F. Zetti,²⁷ and S. Zucchelli²
(CDF Collaboration)

¹Argonne National Laboratory, Argonne, Illinois 60439

²Istituto Nazionale di Fisica Nucleare, University of Bologna, I-40127 Bologna, Italy

³Brandeis University, Waltham, Massachusetts 02254

⁴University of California at Los Angeles, Los Angeles, California 90024

⁵University of Chicago, Chicago, Illinois 60637

⁶Duke University, Durham, North Carolina 27708

⁷Fermi National Accelerator Laboratory, Batavia, Illinois 60510

⁸University of Florida, Gainesville, Florida 32611

⁹Laboratori Nazionali di Frascati, Istituto Nazionale di Fisica Nucleare, I-00044 Frascati, Italy

¹⁰University of Geneva, CH-1211 Geneva 4, Switzerland

¹¹Harvard University, Cambridge, Massachusetts 02138

¹²Hiroshima University, Higashi-Hiroshima 724, Japan

¹³University of Illinois, Urbana, Illinois 61801

¹⁴Institute of Particle Physics, McGill University, Montreal, Canada H3A 2T8

and University of Toronto, Toronto, Canada M5S 1A7

¹⁵The Johns Hopkins University, Baltimore, Maryland 21218

¹⁶Institut für Experimentelle Kernphysik, Universität Karlsruhe, 76128 Karlsruhe, Germany

¹⁷National Laboratory for High Energy Physics (KEK), Tsukuba, Ibaraki 305, Japan

¹⁸Ernest Orlando Lawrence Berkeley National Laboratory, Berkeley, California 94720

¹⁹Massachusetts Institute of Technology, Cambridge, Massachusetts 02139

²⁰University of Michigan, Ann Arbor, Michigan 48109

²¹Michigan State University, East Lansing, Michigan 48824

²²University of New Mexico, Albuquerque, New Mexico 87131

²³The Ohio State University, Columbus, Ohio 43210

²⁴Osaka City University, Osaka 588, Japan

²⁵Università di Padova, Istituto Nazionale di Fisica Nucleare, Sezione di Padova, I-35131 Padova, Italy

²⁶University of Pennsylvania, Philadelphia, Pennsylvania 19104

²⁷Istituto Nazionale di Fisica Nucleare, University and Scuola Normale Superiore of Pisa, I-56100 Pisa, Italy

²⁸University of Pittsburgh, Pittsburgh, Pennsylvania 15260

²⁹Purdue University, West Lafayette, Indiana 47907

³⁰University of Rochester, Rochester, New York 14627

³¹Rockefeller University, New York, New York 10021

³²Rutgers University, Piscataway, New Jersey 08855

³³Academia Sinica, Taipei, Taiwan 11530, Republic of China

³⁴Texas A&M University, College Station, Texas 77843

³⁵Texas Tech University, Lubbock, Texas 79409

³⁶Istituto Nazionale di Fisica Nucleare, University of Trieste, Udine, Italy

³⁷University of Tsukuba, Tsukuba, Ibaraki 315, Japan

³⁸Tufts University, Medford, Massachusetts 02155

³⁹Waseda University, Tokyo 169, Japan

⁴⁰University of Wisconsin, Madison, Wisconsin 53706

⁴¹Yale University, New Haven, Connecticut 06520

(Received 26 August 1998)

We have searched for the decays $B_s^0 \rightarrow e^\pm \mu^\mp$ and $B_d^0 \rightarrow e^\pm \mu^\mp$ using a 102 pb^{-1} data sample of $p\bar{p}$ collisions at $\sqrt{s} = 1.8 \text{ TeV}$ collected with the Collider Detector at Fermilab. We set upper limits on the branching fractions of $\mathcal{B}(B_s^0 \rightarrow e^\pm \mu^\mp) < 6.1(8.2) \times 10^{-6}$ and $\mathcal{B}(B_d^0 \rightarrow e^\pm \mu^\mp) < 3.5(4.5) \times 10^{-6}$ at 90(95)% confidence level. Using these limits, we set lower bounds on the corresponding Pati-Salam leptoquark masses and find that $M_{LQ}(B_s^0) > 20.7(19.3) \text{ TeV}/c^2$ and $M_{LQ}(B_d^0) > 21.7(20.4) \text{ TeV}/c^2$ at 90(95)% confidence level. [S0031-9007(98)08025-9]

Within the standard model the decays $B_s^0 \rightarrow e^\pm \mu^\mp$ and $B_d^0 \rightarrow e^\pm \mu^\mp$ are forbidden by lepton flavor conservation; observation of either of these decays would be evidence for new physics. In particular the assumption of a local gauge symmetry between quarks and leptons leads to the prediction of a new force of nature that mediates transitions between quarks and leptons. One of the simplest models that incorporates this idea is the Pati-Salam model [1] based on the group $SU(4)_c$ where the lepton number is the fourth “color.” At some high-energy scale, the group $SU(4)_c$ is spontaneously broken to $SU(3)_c$, liberating the leptons from the influence of the strong interaction and breaking the symmetry between quarks and leptons. This model predicts heavy spin-one gauge bosons called Pati-Salam leptoquarks (LQ) that carry both color and lepton quantum numbers. The lepton and quark components are not necessarily from the same generation and can mediate the decays $B_s^0 \rightarrow e^\pm \mu^\mp$ and $B_d^0 \rightarrow e^\pm \mu^\mp$ [2,3]. The decay $B_s^0 \rightarrow e^\pm \mu^\mp$ probes two types of LQ: (1) a leptoquark coupling the electron with the b quark and the muon with the s quark; (2) a leptoquark coupling the electron with the s quark and the muon with the b quark. Similarly, $B_d^0 \rightarrow e^\pm \mu^\mp$ probes two different types of LQ.

The current best limits on the branching fractions $\mathcal{B}(B_s^0 \rightarrow e^\pm \mu^\mp)$ and $\mathcal{B}(B_d^0 \rightarrow e^\pm \mu^\mp)$ are $4.1(5.3) \times 10^{-5}$ at 90(95)% confidence level (C.L.) and 5.9×10^{-6} at 90% C.L., set by the L3 [4] and CLEO [5] Collaborations, respectively. We present more stringent limits on both $\mathcal{B}(B_s^0 \rightarrow e^\pm \mu^\mp)$ and $\mathcal{B}(B_d^0 \rightarrow e^\pm \mu^\mp)$, and limits on the corresponding leptoquark masses $M_{\text{LQ}}(B_s^0)$ and $M_{\text{LQ}}(B_d^0)$, using a data sample of 102 pb^{-1} of $p\bar{p}$ collisions at $\sqrt{s} = 1.8 \text{ TeV}$ collected during 1992–1995 with the Collider Detector at Fermilab (CDF).

The CDF detector has been described in detail elsewhere [6]. We briefly describe here those aspects of the detector relevant to this analysis. The tracking system is immersed in a 1.4 T solenoidal magnetic field. The innermost tracking device is a silicon microstrip vertex detector (SVX) [7] that provides spatial measurements in the $r\phi$ [8] plane. The impact parameter [9] resolution of the SVX is $13 + 40/p_T \mu\text{m}$ where p_T is the transverse momentum of the track in GeV/c .

Surrounding the SVX is the central tracking chamber (CTC), which extends out to a radius of 1.3 m and covers the pseudorapidity interval $|\eta| < 1.0$. Combined, the CTC and SVX provide a p_T resolution of $\delta p_T/p_T = \sqrt{(0.9 p_T)^2 + (6.6)^2} \times 10^{-3}$, where p_T is in GeV/c . Electromagnetic (CEM) and hadronic (CHA) calorimeters covering $|\eta| < 1.1$ are located outside the solenoid. A layer of proportional chambers (CES) is embedded in the CEM near shower maximum and measures the shower profile and position. Three muon subsystems in the central region are used. The central muon system (CMU) is located outside the hadron calorimeter and covers the region $|\eta| < 0.6$. The central muon upgrade

system (CMP) is located outside the CMU behind an additional steel absorber. Finally, the central muon extension system (CMX) extends the coverage up to pseudorapidity $|\eta| = 1.0$.

A three-level trigger selects the $e\mu$ candidate events used in this analysis. To be able to predict the signal rate, we require that our candidates satisfy specific triggers at each level. At level 1 we require the presence of a track segment in the CMU or the CMX and an electromagnetic energy deposit (EM cluster) in the CEM. At level 2 we require that the muon track and the EM cluster have matching charged tracks in the CTC found with the Central Fast Track processor [10]. The combined efficiency of the level 1 and level 2 trigger for finding CMU muons rises from 80% at $p_T(\mu) = 3.0 \text{ GeV}/c$ to a plateau efficiency of 87% at $p_T(\mu) = 3.3 \text{ GeV}/c$. The combined efficiency of the level 1 and level 2 trigger for finding CMX muons rises from 50% at $p_T(\mu) = 3.0 \text{ GeV}/c$ to a plateau efficiency of 70% at $p_T(\mu) = 5.0 \text{ GeV}/c$. The combined efficiency of the level 1 and level 2 trigger for finding electrons rises from 15% at $E_T(e) = 5.0 \text{ GeV}$ to a plateau efficiency of 90% for $E_T(e) > 6.5 \text{ GeV}$. The level 3 software trigger requires the presence of a CEM electron with $p_T(e) > 3 \text{ GeV}/c$ and $E_T(e) > 5 \text{ GeV}$ and the presence of a muon with $p_T(\mu) > 3.0 \text{ GeV}/c$ in the CMU or CMX (1992–1993 run) or with $p_T(\mu) > 2.5 \text{ GeV}/c$ in the CMU + CMP or CMX (1994–1995 run).

The signature of the signal is an isolated oppositely charged $e\mu$ pair with an invariant mass consistent with a B meson, where B denotes B_s^0 or B_d^0 in this Letter. The $e\mu$ invariant mass ($m_{e\mu}$) is calculated after constraining the two tracks to come from a common point in space. Candidates failing the fit procedure are discarded. Figure 1 shows the $m_{e\mu}$ distribution for candidates with $5 < m_{e\mu} < 6 \text{ GeV}/c^2$. The distribution is flat indicating a substantial level of combinatorial background. We reduce the background by applying the proper decay length (λ), pointing angle ($\Delta\varphi$), and isolation (I) requirements, which are described below. Table I summarizes the acceptance, trigger efficiencies, and the efficiencies of the off-line analysis requirements.

We use a Monte Carlo simulation to estimate the acceptance listed in row 1 of Table I. We generate b quarks according to a next-to-leading order QCD calculation [11] with minimum b quark $p_T > 5.5 \text{ GeV}/c$ and rapidity $|y(b)| < 1.3$. We use the normalization scale $\mu_0 = \sqrt{m_b^2 + p_T^2}$, a b -quark mass $m_b = 4.75 \text{ GeV}/c^2$, and the MRSD₀ parton distribution functions [12]. The b quarks are fragmented into B mesons using the Peterson parametrization [13] with the fragmentation parameter value of 0.006. The B mesons are forced to decay into $e\mu$. The response of the CDF detector, including the triggers, is then simulated. The acceptance is normalized to B mesons with $p_T(B) > 6 \text{ GeV}/c$ and rapidity $|y(B)| < 1.0$ for which the production cross section is

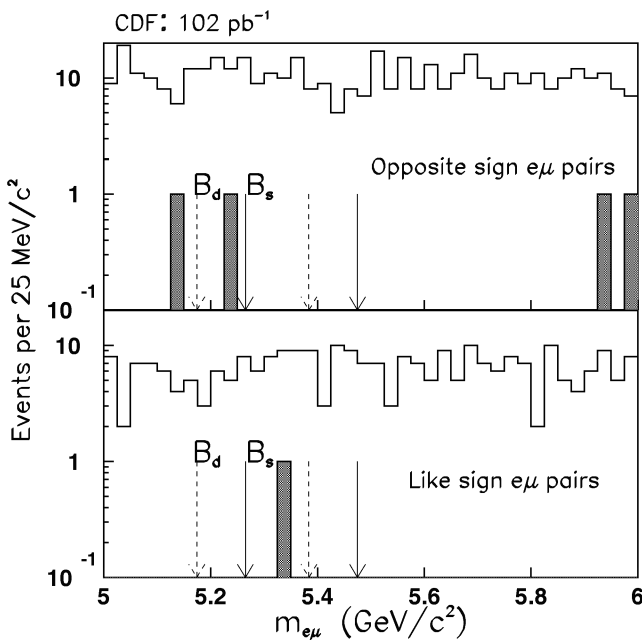


FIG. 1. Invariant mass distribution of opposite-sign (OS) and like-sign (LS) $e\mu$ pairs before and after the λ , $\Delta\varphi$, and I requirements. The arrows indicate the mass windows for B_d^0 (5.279 ± 0.105 GeV/c^2) and B_s^0 (5.370 ± 0.105 GeV/c^2).

measured [14]. The acceptance includes the geometric acceptance as well as the kinematic requirements: $p_T(\mu) > 3.0$ GeV/c , $E_T(e) > 5$ GeV , and $p_T(e\mu) > 6.0$ GeV/c , where $p_T(e\mu)$ is the transverse momentum of the $e\mu$ pair. The overall trigger efficiency is 37.2% for signal events within the geometrical and kinematical acceptance described above. This overall efficiency includes a prescale factor of 65%. The efficiency of reconstructing a track in the CTC (CTC track) has been estimated by embedding two Monte Carlo generated tracks into real data J/ψ events [15].

Muon candidates are selected as follows: the separation between the track in the muon chamber and the extrapolation

TABLE I. Efficiencies and their uncertainties (statistical and systematic uncertainties are added in quadrature). The total efficiency is the product of the individual efficiencies when applied in that order.

| Requirement | Efficiency (%) |
|--|-------------------|
| Geometric and kinematic acceptance for $p_T(B) > 6$ GeV/c and rapidity $ y(B) < 1$ | 2.27 ± 0.024 |
| Trigger efficiency | 37.2 ± 1.6 |
| Reconstruction of two tracks in CTC | 89.8 ± 3.6 |
| Muon selection criteria | 99.5 ± 0.1 |
| Electron selection criteria | 84.8 ± 1.1 |
| Track and vertex quality selection criteria | 68.3 ± 3.1 |
| Proper decay length ($\lambda > 100$ μm) | 81.0 ± 0.8 |
| Pointing angle ($\Delta\varphi < 0.1$) | 85.2 ± 2.3 |
| Isolation ($I > 0.7$) | 85.1 ± 3.0 |
| Mass window | 98.0 ± 0.6 |
| Total efficiency \times acceptance (ϵ_{tot}) | 0.252 ± 0.022 |

lated CTC track is calculated in both the transverse and longitudinal planes. In each view, the difference is required to be less than 3.0 standard deviations (σ), where σ accounts for multiple scattering and measurement uncertainties. Electrons are identified by requiring that the longitudinal profile is consistent with an electron shower, i.e., small leakage in the CHA. The lateral shower profiles as measured with the CEM and CES are required to be consistent with test beam data. The CTC track is required to match the position of the calorimeter shower. Further details on electron identification are described in [16]. The efficiencies of the electron and muon selection criteria are measured using $J/\psi \rightarrow e^+e^-$ and $J/\psi \rightarrow \mu^+\mu^-$ data, respectively.

We exploit the long lifetime of B mesons to reject short-lived combinatorial background. This requires a precise measurement of the B meson decay length. For this reason, both the electron and muon are required to be reconstructed in the SVX, with hits in at least three of the four layers. The uncertainty on the transverse decay length, $L_{xy} = \vec{l}_{xy} \cdot \vec{p}_T(e\mu)/p_T(e\mu)$, is required to be < 200 μm , where \vec{l}_{xy} is the vector pointing from the primary vertex (the interaction point) to the secondary vertex (the reconstructed decay position) in the transverse plane, and $\vec{p}_T(e\mu)$ is the transverse momentum vector of the $e\mu$ pair. The mean uncertainty of L_{xy} is ≈ 60 μm , which is significantly smaller than the mean transverse decay length of ≈ 1.1 mm expected for the signal. We require the proper decay length $\lambda > 100$ μm , where $\lambda = L_{xy} \cdot m_B/p_T(e\mu)$, and m_B is the mass of the B_d^0 or B_s^0 meson. The efficiency of this requirement is studied using Monte Carlo simulation.

The pointing angle $\Delta\varphi$ is defined as the angle between \vec{l}_{xy} and $\vec{p}_T(e\mu)$. For $e\mu$ pairs coming from the decay of a B , \vec{l}_{xy} should point in the same direction as $\vec{p}_T(e\mu)$. Since we require $\lambda > 100$ μm , the direction of \vec{l}_{xy} is well defined. The distribution of $\Delta\varphi$ for opposite-sign $B \rightarrow e^\pm\mu^\mp$ Monte Carlo events (signal) and for like-sign $e\mu$ events (background) with $5 < m_{e\mu} < 6$ GeV/c^2 and $\lambda > 100$ μm is shown in Fig. 2a. We require $\Delta\varphi < 0.1$.

Because of the hard b -quark fragmentation, B mesons carry most of the transverse momentum of the b quark and are isolated. The isolation is defined as $I = p_T(e\mu)/p_T(e\mu) + \sum p_T$, where $\sum p_T$ is the scalar sum of the transverse momenta of all tracks excluding the e and μ within a cone of $\Delta R < 1$ [where $\Delta R = \sqrt{(\Delta\eta)^2 + (\Delta\phi)^2}$] around the momentum vector of the $e\mu$ pair. The z coordinate of these tracks at the closest approach to the beam line must be within 5 cm of the B candidate vertex to exclude tracks from other $p\bar{p}$ collisions that can occur during the same bunch crossing. We require $I > 0.7$. The efficiency of the isolation requirement is obtained using a data sample of fully reconstructed $B^\pm \rightarrow J/\psi K^\pm$ and $B^0 \rightarrow J/\psi K^{*0}$ events. The distribution of the isolation variable for (sideband subtracted) $B^\pm \rightarrow J/\psi K^\pm$ and $B^0 \rightarrow J/\psi K^{*0}$

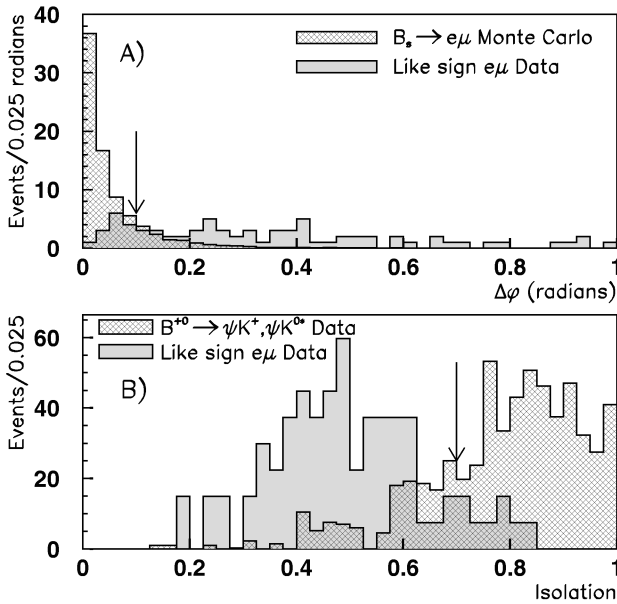


FIG. 2. (a) Distribution of the pointing variable $\Delta\phi$ for Monte Carlo events (signal) and for LS $e\mu$ events (background) with $5 < m_{e\mu} < 6 \text{ GeV}/c^2$ and $\lambda > 100 \mu\text{m}$. (b) Distribution of the isolation variable for sideband subtracted $B^\pm \rightarrow J/\psi K^\pm$ and $B^0 \rightarrow J/\psi K^{*0}$ events (signal) compared to the isolation of LS $e\mu$ events (background) with $5 < m_{e\mu} < 6 \text{ GeV}/c^2$ and $\lambda > 100 \mu\text{m}$. The arrows in both cases indicate the cut values. In both plots the two distributions are normalized to the same total number of entries.

events (signal) compared to the isolation of LS $e\mu$ events (background) with $5 < m_{e\mu} < 6 \text{ GeV}/c^2$ and $\lambda > 100 \mu\text{m}$ is shown in Fig. 2b.

The λ , $\Delta\phi$, and I requirements have been optimized by maximizing the signal-to-background significance, ϵ_S^2/ϵ_B , where ϵ_S is the efficiency for $B \rightarrow e^\pm \mu^\mp$ events and ϵ_B is the efficiency for background events. To estimate ϵ_B we use LS $e\mu$ pairs in the 5–6 GeV/c^2 mass range as a sample of background.

Fully reconstructed $B \rightarrow e^\pm \mu^\mp$ events from a Monte Carlo simulation are used to estimate the mass resolution and the efficiency of the mass window requirements. We find a resolution of 33 MeV/c^2 and define the mass windows of $5.279 \pm 0.105 \text{ GeV}/c^2$ for the B_d^0 and $5.370 \pm 0.105 \text{ GeV}/c^2$ for the B_s^0 . The uncertainty of the efficiency of the mass window requirement is estimated by varying the mass resolution by $\pm 10\%$.

Figure 1 shows the $m_{e\mu}$ distributions for OS and LS $e\mu$ pairs before and after the λ , $\Delta\phi$, and I requirements. We observe 422 OS and 262 LS events for $5 < m_{e\mu} < 6 \text{ GeV}/c^2$ before the requirements, as we expect more OS events from $b\bar{b}$ pair production. These numbers are reduced to 85 OS and 58 LS events after the λ requirement, 16 OS and 12 LS events after the $\Delta\phi$ requirement, and, finally, 4 OS and 1 LS events after the I requirement. One OS event remains in the B_d^0 mass window, while no candidates are found in the B_s^0 mass window. From LS events we estimate 0.2 ± 0.2 background events in the signal region and from OS

events outside of the B^0 mass window we estimate 0.8 ± 0.5 background events.

As there is no evidence for a signal we proceed to set limits. When setting limits we make no background subtraction and take into account the systematic uncertainties on the B_d^0 meson measured cross section (23%) [14], the efficiency and acceptance (10%), and the integrated luminosity (7%). We obtain $N^l(B_d^0 \rightarrow e^\pm \mu^\mp) = 4.34(5.52)$ events and $N^l(B_s^0 \rightarrow e^\pm \mu^\mp) = 2.52(3.38)$ events at 90(95%) C.L., where N^l is the upper limit on the number of events. We determine the limits on $\mathcal{B}(B \rightarrow e^\pm \mu^\mp)$ for B_s^0 and B_d^0 using the following relationship between N^l and the branching fraction:

$$2\sigma(B)\mathcal{B}(B \rightarrow e^\pm \mu^\mp) < \frac{N^l(B \rightarrow e^\pm \mu^\mp)}{\int \mathcal{L} dt \epsilon_{\text{tot}}}.$$

The factor of 2 takes into account that we do not distinguish B and \bar{B} decays. We assume $\sigma(B_s^0) = 1/3 \times \sigma(B_d^0)$ [17] and use $\sigma(B_d^0)[p_T(B) > 6 \text{ GeV}/c, |y(B)| < 1.0] = 2.39 \pm 0.32 \pm 0.44 \mu\text{b}$ [14], $\int \mathcal{L} dt = 102 \text{ pb}^{-1}$ and the total efficiency (ϵ_{tot}) value listed in Table I. We obtain the following upper bounds at 90(95%) C.L.:

$$\mathcal{B}(B_s^0 \rightarrow e^\pm \mu^\mp) < 6.1(8.2) \times 10^{-6} \text{ and}$$

$$\mathcal{B}(B_d^0 \rightarrow e^\pm \mu^\mp) < 3.5(4.5) \times 10^{-6}.$$

The relationship between the branching ratio $\mathcal{B}(B_s^0 \rightarrow e^\pm \mu^\mp)$ [similarly for the $\mathcal{B}(B_d^0 \rightarrow e^\pm \mu^\mp)$ case] and the corresponding M_{LQ} is as follows [2]:

$$\Gamma(B_s^0 \rightarrow e\mu) = \pi \alpha_s^2(M_{\text{LQ}}) \frac{1}{M_{\text{LQ}}^4} F_{B_s^0}^2 m_{B_s^0}^3 R^2$$

where

$$R = \frac{m_{B_s^0}}{m_b} \left(\frac{\alpha_s(M_{\text{LQ}})}{\alpha_s(m_t)} \right)^{-4/7} \left(\frac{\alpha_s(m_t)}{\alpha_s(m_b)} \right)^{-12/23}.$$

We use $F_{B_d^0} = 175 \pm 30 \text{ MeV}$ for the B_d^0 decay constant [18]. $F_{B_s^0}$ is derived from $F_{B_d^0}$ using the following relationship obtained from lattice QCD [18]: $F_{B_s^0}/F_{B_d^0} = 1.14 \pm 0.05$ resulting in $F_{B_s^0} = 200 \pm 35 \text{ MeV}$. For the other quantities we use values [19] $m_{B_s^0} = 5.3696 \pm 0.0024 \text{ GeV}/c^2$ for the B_s^0 meson mass, $m_{B_d^0} = 5.2792 \pm 0.0018 \text{ GeV}/c^2$ for the B_d^0 meson mass, $m_b = 4.3 \pm 0.2 \text{ GeV}/c^2$ for the b -quark mass, $\tau_{B_s^0} = 1.57 \pm 0.08 \text{ ps}$ for the B_s^0 lifetime, $\tau_{B_d^0} = 1.55 \pm 0.05 \text{ ps}$ for the B_d^0 lifetime, and $m_t = 175.9 \pm 6.9 \text{ GeV}/c^2$ [20] for the top quark mass. We use $\alpha_s(M_Z) = 0.115$ which is evolved to M_{LQ} using the Marciano approximation [21], assuming no colored particles lie between m_t and M_{LQ} . We obtain the following bounds on the masses of the corresponding LQ at 90(95%) C.L.:

$$M_{\text{LQ}}(B_s^0) > 20.7(19.3) \text{ TeV}/c^2 \text{ and}$$

$$M_{\text{LQ}}(B_d^0) > 21.7(20.4) \text{ TeV}/c^2.$$

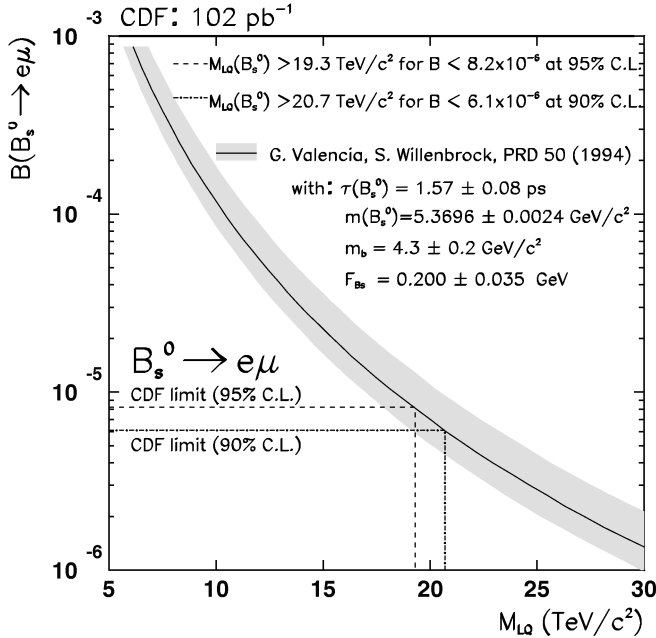


FIG. 3. Pati-Salam leptoquark mass limits corresponding to the 90(95)% C.L. limits on $\mathcal{B}(B_s^0 \rightarrow e^\pm \mu^\mp)$. The error band represents the theoretical uncertainties.

The limits for the B_s^0 case and the theoretical prediction for $M_{LQ}(B_s^0)$ as a function of $\mathcal{B}(B_s^0 \rightarrow e^\pm \mu^\mp)$ are shown in Fig. 3.

In conclusion we have searched for the decays $B_s^0 \rightarrow e^\pm \mu^\mp$ and $B_d^0 \rightarrow e^\pm \mu^\mp$. No evidence is found for these decays. We set upper limits on the branching fractions and lower limits on the corresponding Pati-Salam leptoquark masses.

We thank S. Willenbrock for motivating us to do this analysis and for his contribution to the theoretical interpretation. We thank the Fermilab staff and the technical staffs of the participating institutions for their vital contributions. This work was supported by the U.S. Department of Energy and National Science Foundation, the Italian Istituto Nazionale di Fisica Nucleare, the Ministry of Education, Science and Culture of Japan, the Natural Sciences and Engineering Research Council of Canada, the National Science Council of the Republic of China, the Swiss National Science Foundation, and the A.P. Sloan Foundation.

*Visitor.

- [1] J. Pati and A. Salam, Phys. Rev. D **10**, 275 (1974).
- [2] G. Valencia and S. Willenbrock, Phys. Rev. D **50**, 6843 (1994). This paper also discusses leptoquark mass limits derived from K and π decays.
- [3] A. V. Kuznetsov and N. V. Mikheev, Phys. Lett. B **329**, 295 (1994).
- [4] M. Acciarri *et al.*, Phys. Lett. B **391**, 474 (1997).
- [5] R. Ammar *et al.*, Phys. Rev. D **49**, 5701 (1994).
- [6] F. Abe *et al.*, Nucl. Instrum. Methods Phys. Res., Sect. A **271**, 387 (1988).
- [7] D. Amidei *et al.*, Nucl. Instrum. Methods Phys. Res., Sect. A **350**, 73 (1994).
- [8] In CDF the positive z (longitudinal) axis lies along the proton beam direction, r is the radius from this axis, θ is the polar angle, and ϕ is the azimuthal angle. Pseudorapidity (η) is defined as $\eta = -\ln[\tan(\theta/2)]$. E_T and p_T are the energy flow and the momentum measured transverse to the beam line, respectively.
- [9] The impact parameter is the distance of closest approach of the track helix to the beam axis, measured in the transverse plane.
- [10] G. W. Foster *et al.*, Nucl. Instrum. Methods Phys. Res., Sect. A **269**, 93 (1988).
- [11] P. Nason, S. Dawson, and R. Ellis, Nucl. Phys. **B326**, 49 (1988); P. Dawson *et al.*, Nucl. Phys. **B327**, 49 (1988); M. Mangano *et al.*, Nucl. Phys. **B373**, 295 (1992).
- [12] A. Martin, J. Stirling, and R. Roberts, Phys. Rev. D **47**, 867 (1993).
- [13] C. Peterson *et al.*, Phys. Rev. D **27**, 105 (1983).
- [14] F. Abe *et al.*, Phys. Rev. Lett. **75**, 1451 (1995).
- [15] F. Abe *et al.*, Phys. Rev. D **58**, 072001 (1998).
- [16] F. Abe *et al.*, Phys. Rev. D **52**, 2624 (1995).
- [17] 1/3 is consistent with the measurement of $0.34 \pm 0.10 \pm 0.03$: F. Abe *et al.*, Phys. Rev. D **54**, 6596 (1996).
- [18] C. Bernard, in Proceedings of the 7th International Symposium on Heavy Flavor Physics, Santa Barbara, CA, 1997 (hep-ph/9709460, and references therein).
- [19] Particle Data Group, R. M. Barnett *et al.*, Phys. Rev. D **54**, 1 (1996); 1997 off-year partial update for the 1998 edition available on the PDG WWW pages (URL: <http://pdg.lbl.gov/>).
- [20] F. Abe *et al.*, Phys. Rev. Lett. **80**, 2767 (1998).
- [21] W. Marciano, Phys. Rev. D **29**, 580 (1984).